



A Case of Cisternal Pilocytic Astrocytoma Diagnosed with the Balanced Steady-State Free Precession Sequence for Magnetic Resonance Imaging: A Rare Cause of Subarachnoid Hemorrhage

Taro Suzuki¹, Yosuke Akamatsu¹, Sotaro Oshida¹, Kenta Aso¹, Mitsumasa Osakabe², Hiroshi Kashimura¹

Key words

- Balanced steady-state free precession sequence
- Cistern
- Pilocytic astrocytoma
- Subarachnoid hemorrhage
- Unknown etiology

Abbreviations and Acronyms

bSSFP: Balanced steady-state free precession

CT: Computed tomography

MRI: Magnetic resonance imaging

PA: Pilocytic astrocytoma

SAH: Subarachnoid hemorrhage

From the ¹Department of Neurosurgery, Iwate Prefectural Chubu Hospital, Kitakami; and ²Department of Molecular Diagnostic Pathology, Iwate Medical University, Uchimarui, Morioka, Iwate, Japan

To whom correspondence should be addressed:

Yosuke Akamatsu, M.D.

[E-mail: redpine7219@gmail.com]

Citation: *World Neurosurg.* X (2019) 1:100003.

<https://doi.org/10.1016/j.wnsx.2018.100003>

Journal homepage: www.journals.elsevier.com/world-neurosurgery-x

Available online: www.sciencedirect.com

2590-1397/© 2019 The Authors. Published by Elsevier Inc. This is an open access article under the CC BY-NC-ND license (<http://creativecommons.org/licenses/by-nc-nd/4.0/>).

INTRODUCTION

Pilocytic astrocytoma (PA) is a World Health Organization grade I tumor typically seen in the pediatric population.¹ In general, tumor-related hemorrhage is higher in high-grade glioma than in low-grade glioma. However, many studies have demonstrated that PA presents as intratumoral hemorrhage with a greater frequency than previously thought.²⁻³ In addition, dissemination from the initial tumor has been observed as an atypical feature.^{4,5} A rare case of cisternal PA without intraparenchymal mass formation presenting as subarachnoid hemorrhage (SAH) is described in this article. The usefulness of fast imaging with balanced steady-state free precession (bSSFP) magnetic resonance imaging (MRI) to detect

■ **OBJECTIVES:** In approximately 15% of cases of spontaneous subarachnoid hemorrhage (SAH), an obvious source of bleeding cannot be identified by angiography; these are considered cases of SAH of unknown etiology. A rare case of cisternal pilocytic astrocytoma (PA) presenting with SAH is reported. The usefulness of the balanced steady-state free precession (bSSFP) sequence for magnetic resonance imaging (MRI) to detect small cisternal lesions is discussed.

■ **CASE DESCRIPTION:** The case of a 73-year-old woman who developed repeated SAHs owing to a cisternal PA is presented. She experienced sudden onset of headache and vomiting, and brain computed tomography showed diffuse SAH, whereas angiography demonstrated normal vasculature. Follow-up imaging, including T1-weighted, T2-weighted, T1-weighted contrast-enhanced, and diffusion-weighted MRI, did not show any parenchymal or cisternal lesions, although computed tomography and fluid-attenuated inversion recovery MRI showed SAH in the same region. In contrast, the bSSFP sequence, taken as a different sequence on the same day, showed mixed-intensity reticular lesions in the left basal cistern, while neither hematoma nor positive findings were identified with the other sequences. Based on the radiologic finding and the repeated history of SAH, the lesions were partially removed 2 weeks after onset. Histological examination showed a PA.

■ **CONCLUSIONS:** Despite being extremely rare, a small cisternal lesion should be considered as a cause of SAH of unknown etiology. The bSSFP sequence may be useful for detecting cisternal lesions that may be missed on the routine MRI sequences.

the cisternal lesion in cases of SAH of unknown etiology is suggested.

CASE DESCRIPTION

A 73-year-old woman presented with sudden onset of headache and vomiting. Brain computed tomography (CT) showed diffuse SAH (Figure 1). She had experienced SAH of unknown vascular etiology 2 years earlier and had been observed at another hospital. Six-vessel digital subtraction angiography showed no aneurysm or abnormal vascularity (Figure 2). Therefore, the patient was managed conservatively. Follow-up CT and MRI were performed 2 days after

onset. CT demonstrated only residual subarachnoid hematoma in the right basal cistern (Figure 3A). On T1-weighted, T2-weighted, and T1-weighted contrast-enhanced images, no parenchymal or cisternal lesion was apparent (Figure 3B–D). Fluid-attenuated inversion recovery images showed subarachnoid hematoma at the right basal cistern, as shown on CT (Figure 3E). However, the bSSFP sequence (fast imaging employing steady-state acquisition [General Electric, Milwaukee, Wisconsin, USA]) demonstrated mixed-intensity reticular lesions in the left basal cistern, while residual subarachnoid hematoma was not demonstrated (Figure 3F). Based on this finding and the



Figure 1. Computed tomography on the day of admission showing diffuse subarachnoid hemorrhage.

repeated history of SAH, the patient underwent open surgical inspection via a left pterional craniotomy to confirm the underlying pathology. When the proximal Sylvian cistern was opened, the grayish, soft, hemorrhagic component was observed. The tumor occupied the left basal cistern and involved the left internal carotid artery (Figure 4A) and its perforating branches (Figure 4B), although the border between the tumor and the brain parenchyma was clear. Intraoperative rapid pathology indicated no malignancy, suggesting low-grade glioma. A large part of the tumor anterior to the internal carotid artery and optic nerve, including the hemorrhagic component, was partially removed, because radical removal might have caused severe complications associated with injury of the perforating arteries (Figure 4C). Histopathological examination of the tumor showed a typical PA with a

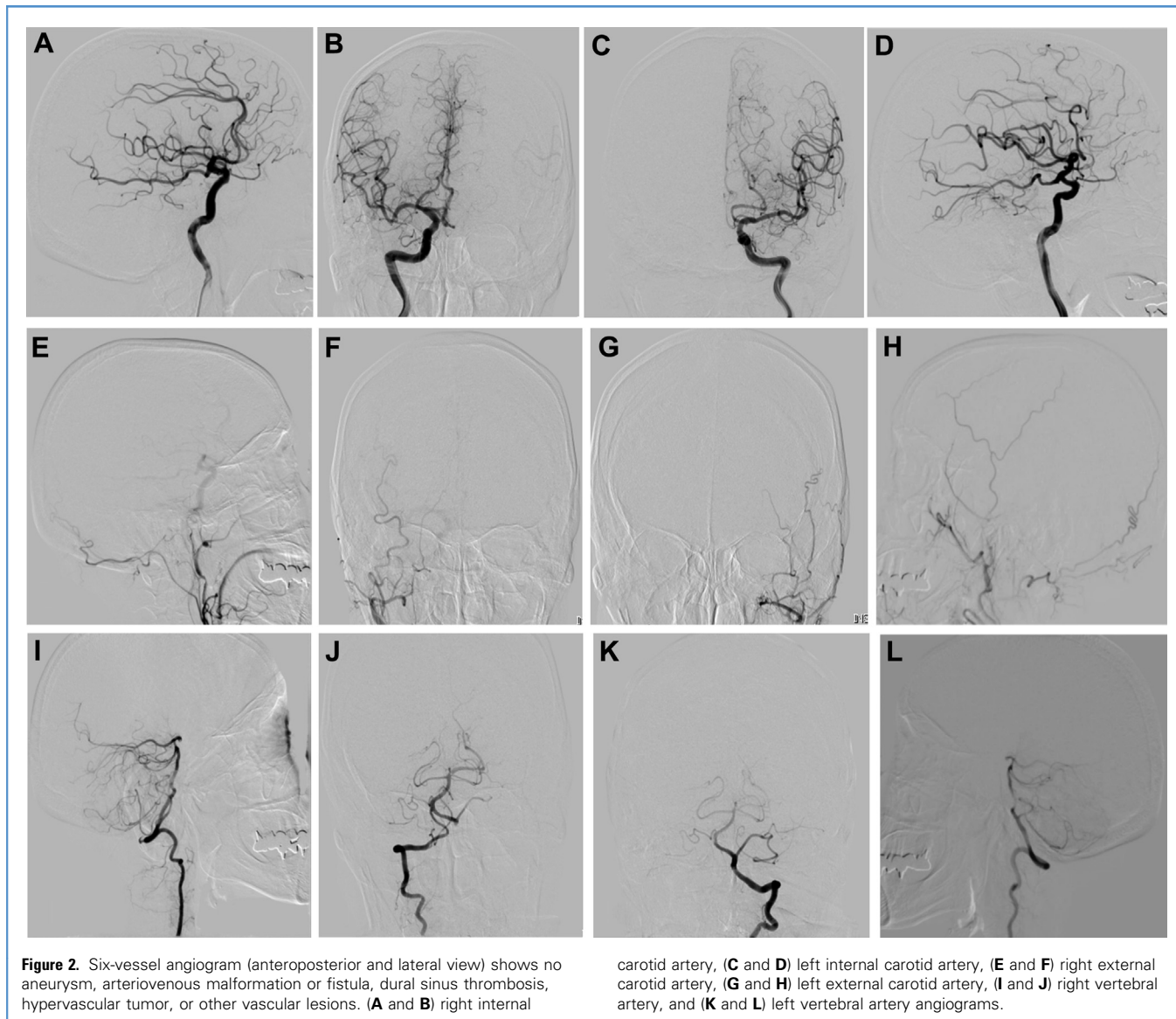
mixture of a compact fibrillary area and microcystic foci (Figure 4D). Subsequent surgical procedures were uneventful. The patient underwent no adjuvant therapy, and her subsequent course has been uneventful without any signs of deterioration to date.

DISCUSSION

Although tumor-related intraparenchymal hemorrhage was observed in between 8%–11% of PAs, a higher incidence than one would expect,^{3,6} SAH is a rare presentation. Only 9 PA cases presenting with SAH, including the present case, have been reported (Table 1).^{2,7–13} The median age of these patients was 30 (range 1–73) years, with a male predominance (77.8%). Except for the present case, 8 of 9 lesions (88.9%) showed mass formation on radiologic examinations, so that the lesions were detected relatively

easily. The tumors were located in the hypothalamus or optic nerve in 8 of 9 cases (88.9%), with 1 case in the cerebellum. In all cases, the tumors were adjacent to the subarachnoid space, as expected. Because of its vital location and potential involvement with cranial nerves, the internal carotid artery, and its branches, total removal was not achieved in 7 of 9 cases (77.8%).

Although hemorrhagic onset of PA is not as rare as was previously thought, the related mechanisms remain unclear. Pathological findings in cases of hemorrhagic PA showed nonspecific degenerative change in intratumoral vessels and no difference in proliferation of tumor and microvasculature compared to non-hemorrhagic PA.^{2,3} The age distribution of patients with hemorrhagic PA tends to be older than that of patients with non-hemorrhagic PA.³ This older-age predominance was seen in the PA patients



presenting with SAH as well. Therefore, because PAs are slow-growing tumors and might be incidentally detected in adults, degenerative changes in intratumoral vessels in long-standing PAs might be related to the onset of SAH.

PAs seems to be the exception to the rule of low-grade neoplasm owing to some inconsistent aspects. PAs sometimes have a ring-enhancement pattern, which is seen in high-grade glioma, as well as the classic pattern of the cyst-like mass with an enhancing mural nodule.¹⁴ Furthermore, previous studies demonstrated that

leptomeningeal dissemination of PAs occurs in about 2%–12% of cases, with a higher incidence if the tumors are located at the hypothalamus or chiasma.¹⁵ However, if the tumor does not show mass formation on routine images and the patient is asymptomatic, the lesions may be underestimated and undiagnosed, as in the present case. In the present patient, the disseminated lesion was visible only on the bSSFP sequence, not on the other routine sequences, including the postcontrast T₁ sequence. The bSSFP sequence is now

freely available and useful when routine MRI sequences cannot provide desired anatomic information. This sequence provides a high signal in tissues with a high signal-to-noise ratio and enables submillimeter spatial resolution, and it is effective for detecting lesions in the cisternal space, cavernous sinuses, and the ventricular system, where it is useful for detecting subtle cerebrospinal fluid-intensity lesions that may be missed on routine spin-echo sequences.¹⁶ Furthermore, Abele et al.¹⁷ reported that modification of the basic bSSFP

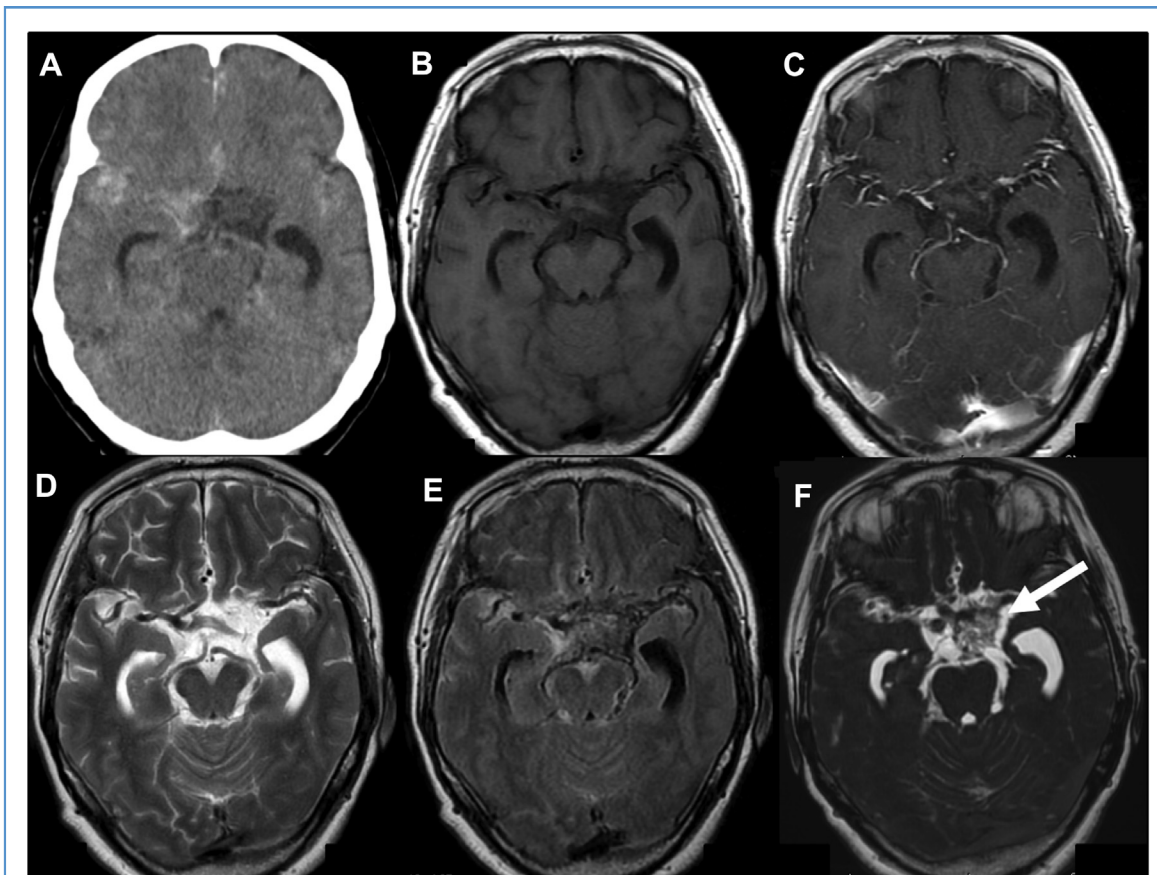


Figure 3. (A) Follow-up computed tomography (CT) scan 2 days after onset showing residual subarachnoid hematoma in the right basal cistern. Magnetic resonance imaging scan at the level of the basal cistern, obtained 2 days after onset, demonstrating no intraparenchymal lesion or cisternal lesion on axial T1-weighted noncontrast (B), T1-weighted contrast (C),

T2-weighted images (D). Fluid-attenuated inversion recovery image showing residual subarachnoid hematoma, consistent with the findings of the CT scan (E). In contrast, the balanced steady-state free precession image demonstrating the mixed-intensity reticular lesions in the left basal cistern (arrow) (F).

sequence can detect even small subcentimeter internal auditory canal lesions, which have been considered by many to require gadolinium administration for detection. Buch et al.¹⁸ also reported the utility of the bSSFP sequence for small drop metastases (<3 mm) and nonenhancing metastases. In addition to these reports, we suggest that the bSSFP sequence should be performed, as well as routine sequences, in cases of SAH without obvious vascular etiology.

Treatment of PAs varies depending on the location of the tumors and the clinical manifestations. Surgical removal should be performed as radical therapy if the tumors arise from a removable region.¹⁹ However, if the tumor involves the optic

pathway, hypothalamus, or surrounding vascular structures, the treatment of PA can be divided into observation, chemotherapy, radiation therapy, and surgery.²⁰ In patients who have symptoms of visual loss, endocrine disturbance, hydrocephalus, or mass effect, aggressive intervention should be considered. The main role of surgery is to confirm the histological diagnosis and decompress the mass without postoperative neurologic deterioration. The effect of radiation therapy and chemotherapy in adult PAs remains unknown given the small number of patients treated. However, for patients who have small tumors and are asymptomatic, careful observation may be considered.²¹ In the present case, evacuation of the hematoma in conjunction with

conservative decompression was performed without adjuvant therapy.

CONCLUSIONS

In conclusion, cisternal lesions should be included in the differential diagnosis of SAH of unknown vascular etiology; bSSFP may be useful for detecting cisternal lesions that may be missed on the other MRI sequences.

Despite being extremely rare, a small cisternal lesion should be considered as a cause of SAH of unknown etiology.

ACKNOWLEDGEMENTS

We thank Forte (<https://www.forte-science.co.jp>) for English language editing.

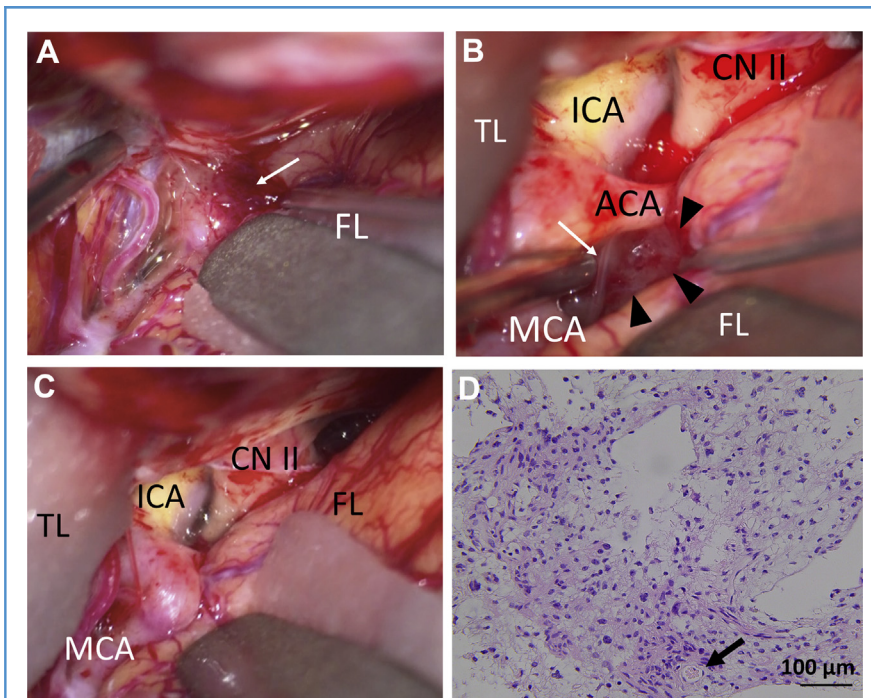


Figure 4. Intraoperative view obtained via the left pterional approach. The tan and gelatinous tumor occupying the left basal cistern. The hemorrhagic component was seen at basal cistern (*white arrow*) (A). High magnification intraoperative view indicating residual tumor (*black arrowheads*) involving the perforating artery originating from the ICA (*white arrow*) (B). The tumor is partially removed, and the middle cerebral artery, internal carotid artery,

and left optic nerve are visible (C). Photomicrograph showing diffusely proliferated astrocytic cells with a microcystic space. Perivascular proliferation of tumor cells (*arrow*) is visible. Hematoxylin-eosin stain, x 200 (D). ACA, anterior cerebral artery; CN II, optic nerve; FL, frontal lobe; ICA, internal carotid artery; MCA, middle cerebral artery; TL, temporal lobe.

Table 1. Summary of Pilocytic Astrocytomas Presenting with Subarachnoid Hemorrhage

Series (Reference Number)	Age (Years)	Sex	Mass Formation	Location of Tumor	Operation
Glew 1977 ⁷	30	Male	Yes	Hypothalamus	Biopsy
Charles et al., 1981 ⁸	45	Male	Yes	Optic nerve	Partial removal
Matsumoto et al., 1997 ⁹	45	Male	Yes	Hypothalamus	Partial removal
Hwang et al., 1998 ¹⁰	34	Male	Yes	Hypothalamus	Total removal
Garg et al., 2004 ¹¹	13	Male	Yes	Hypothalamus	Partial removal
Lee et al., 2009 ¹²	1	Male	Yes	Cerebellum	Partial removal
Shibahara et al., 2009 ²	18	Male	Yes	Hypothalamus	Biopsy
Kato et al., 2011 ¹³	20	Female	Yes	Medial frontal	Total removal
Present case	73	Female	No	Basal cistern	Partial removal

REFERENCES

1. Louis DN, Ohgaki H, Wiestler OD. *The 2007 WHO Classification of Tumors of the Central Nervous System*. Lyon, France: IARC Press; 2007:14-20.
2. Shibahara I, Kanamori M, Kumabe T, et al. Hemorrhagic onset of pilocytic astrocytoma and pilomyxoid astrocytoma. *Brain Tumor Pathol.* 2009; 26:1-5.
3. Shibao S, Kimura T, Sasaki H, et al. Hemorrhagic onset of cerebellar pilocytic astrocytoma in an adult: a case report and review of the literature implying a possible relation of degenerative vascular changes to the massive intratumoral hemorrhage. *Brain Tumor Pathol.* 2012;29:96-102.
4. Chourmouzi D, Papadopoulou E, Konstantinidis M, et al. Manifestations of pilocytic astrocytoma: a pictorial review. *Insights Imaging.* 2014;5:387-402.
5. Linscott LL, Osborn AG, Blaser S, et al. Pilomyxoid astrocytoma: expanding the imaging spectrum. *AJNR Am J Neuroradiol.* 2008;29:1861-1866.
6. White JB, Piepgras DG, Scheithauer BW, Parisi JE. Rate of spontaneous hemorrhage in histologically proven cases of pilocytic astrocytoma. *J Neurosurg.* 2008;108:223-226.
7. Glew WB. Stimulated pituitary apoplexy: report of an unusual case due to hemorrhage into hypothalamic astrocytoma. *Ann Ophthalmol.* 1977;9:139-142.
8. Charles NC, Nelson L, Brookner AR, Lieberman N, Breinin GM. Pilocytic astrocytoma of the optic nerve with hemorrhage and extreme cystic degeneration. *Am J Ophthalmol.* 1981;92:691-695.
9. Matsumoto K, Akagi K, Abekura M, et al. Hypothalamic pilocytic astrocytoma presenting with intratumoral and subarachnoid hemorrhage. *Neurol Med Chir.* 1997;37:849-851.
10. Hwang SL, Huang TY, Chai CY, Howng SL. Hypothalamic juvenile pilocytic astrocytoma presenting with intracerebral hemorrhage. *J Formos Med Assoc.* 1998;97:784-787.
11. Garg A, Chugh M, Gaikwad SB, et al. Juvenile pilocytic astrocytoma presenting with subarachnoid hemorrhage. Case report and review of the literature. *J Neurosurg.* 2004;100:525-529.
12. Lee CS, Huh JS, Sim KB, Kim YW. Cerebellar pilocytic astrocytoma presenting with intratumor bleeding, subarachnoid hemorrhage, and subdural hematoma. *Childs Nerv Syst.* 2009;25:125-128.
13. Kato K, Moteki Y, Nakagawa M, Kadoyama S, Ujiie H. Subarachnoid hemorrhage caused by pilocytic astrocytoma-case report. *Neurol Med Chir.* 2011;51:82-84.
14. Nakano Y, Yamamoto J, Takahashi M, et al. Pilocytic astrocytoma presenting with atypical features on magnetic resonance imaging. *J Neuroradiol.* 2015;42:278-282.
15. Mamelak AN, Prados MD, Obana WG, Cogen PH, Edwards MS. Treatment options and prognosis for multicentric juvenile pilocytic astrocytoma. *J Neurosurg.* 1994;81:24-30.
16. Chávez GD, De Salles AA, Solberg TD, Pedrosa A, Espinoza D, Villablanca P. Three-dimensional fast imaging employing steady-state acquisition magnetic resonance imaging for stereotactic radiosurgery of trigeminal neuralgia. *Neurosurgery.* 2005; 56:E628.
17. Abele TA, Besachio DA, Quigley EP, et al. Diagnostic accuracy of screening MR imaging using unenhanced axial CISS and coronal T2WI for detection of small internal auditory canal lesions. *AJNR Am J Neuroradiol.* 2014;35:2366-2370.
18. Buch K, Caruso P, Ebb D, Rincon S. Balanced steady-state free precession sequence (CISS/FIESTA/3D driven equilibrium radiofrequency reset pulse) increases the diagnostic yield for spinal drop metastases in children with brain tumors. *AJNR Am J Neuroradiol.* 2018;39:1355-1361.
19. Burkhard C, Di Patre PL, Schüler D, et al. A population-based study of the incidence and survival rates in patients with pilocytic astrocytoma. *J Neurosurg.* 2003;98:1170-1174.
20. Binning MJ, Liu JK, Kestle JR, Brockmeyer DL, Walker ML. Optic pathway gliomas: a review. *Neurosurg Focus.* 2007;23:E2.
21. Theeler BJ, Ellezam B, Sadighi ZS, et al. Adult pilocytic astrocytomas: clinical features and molecular analysis. *Neuro Oncol.* 2014;16:841-847.

Conflict of interest statement: The authors declare that the article content was composed in the absence of any commercial or financial relationships that could be construed as a potential conflict of interest.

Received 9 October 2018; accepted 6 December 2018

*Citation: World Neurosurg. X (2019) 1:100003.
<https://doi.org/10.1016/j.wnsx.2018.100003>*

Journal homepage: www.journals.elsevier.com/world-neurosurgery-x

Available online: www.sciencedirect.com

2590-1397/© 2019 The Authors. Published by Elsevier Inc. This is an open access article under the CC BY-NC-ND license (<http://creativecommons.org/licenses/by-nc-nd/4.0/>).